PLANT SCIENCE

Volatile communication in plants relies on a KAI2-mediated signaling pathway

Shannon A. Stirling[1], Angelica M. Guercio[2], Ryan M. Patrick[1,3], Xing-Qi Huang[3,4], Matthew E. Bergman[3,4], Varun Dwivedi[3,4]†, Ruy W. J. Kortbeek[3,4], Yi-Kai Liu[4], Fuai Sun[2], W. Andy Tao[4,5,6,7], Ying Li[1,3], Benoît Boachon[3,4,8], Nitzan Shabek[2], Natalia Dudareva[1,3,4]*

Plants are constantly exposed to volatile organic compounds (VOCs) that are released during plant-plant communication, within-plant self-signaling, and plant-microbe interactions. Therefore, understanding VOC perception and downstream signaling is vital for unraveling the mechanisms behind information exchange in plants, which remain largely unexplored. Using the hormone-like function of volatile terpenoids in reproductive organ development as a system with a visual marker for communication, we demonstrate that a petunia karrikin-insensitive receptor, PhKAI2ia, stereospecifically perceives the (−)-germacrene D signal, triggering a KAI2-mediated signaling cascade and affecting plant fitness. This study uncovers the role(s) of the intermediate clade of KAI2 receptors, illuminates the involvement of a KAI2ia-dependent signaling pathway in volatile communication, and provides new insights into plant olfaction and the long-standing question about the nature of potential endogenous KAI2 ligand(s).

Volatile organic compounds (VOCs) are released by all kingdoms of life, including bacteria and fungi, and mediate intra- and interspecific communications above- and belowground (*1*). Specifically, plant VOCs emitted from aerial organs into the atmosphere and from roots into the soil play key roles in attracting pollinators and other beneficial organisms, defending plants against herbivores and pathogens, and protecting against abiotic stresses (*2*). In addition, plants are constantly exposed to volatiles as a part of plant-plant and plant-microbe interactions, and within-plant signaling (*3*–*5*). Therefore, perception of volatiles and downstream signaling are essential parts of communication, given that receivers must decrypt the chemical language to distinguish signals from background odors and respond to specific VOC cues. Owing to the plethora of biological processes that are dependent on VOCs, substantial progress has been made toward understanding the biosynthesis of plant VOCs and their regulation and, in recent years, the molecular mechanisms involved in VOC emission (*6*–*8*). Yet little is known about how plants perceive VOCs and trigger cellular response(s) that may enhance their resilience and overall fitness.

In animals, VOCs are recognized by odorant receptors in the olfactory neural system, which constitute the largest G protein–coupled receptor (GPCR) family (*9*). By contrast, plants have only a few GPCR proteins that appear to have different functions (*10*). To date, only limited information exists about the receptors for airborne signals in plants. These examples include (i) ETR and NTHK1 receptors for the volatile plant hormone ethylene (*11*, *12*); (ii) salicylic acid-binding protein-2 (SABP2), a receptor for airborne methyl salicylate (*13*); (iii) a KAI2 receptor for volatile karrikins (*14*), which are small bioactive organic compounds produced by wildfires (*15*, *16*); and (iv) TOPLESS-like proteins (TPLs), which are transcriptional cosuppressors with β-caryophyllene–binding activity that are involved in VOC sensing in tobacco (*17*).

The absence of reliable molecular markers of the perception state in receiving plants greatly slowed progress in the investigation of plant olfaction. However, we have recently discovered that in *Petunia hybrida* flowers, volatile terpenoids can move between different organs by natural fumigation (*3*). Produced by terpene synthase 1 (PhTPS1) in flower tubes and released before anthesis inside the buds, sesquiterpenes accumulate in reproductive organs and are required for normal pistil development. Because the loss of sesquiterpene fumigation by down-regulation of *PhTPS1* transcript levels significantly decreases pistil weight and stigma size (*3*), we used this hormone-like function of volatile terpenoids as a visual marker for communication to investigate the molecular mechanisms that underlie VOC perception and signaling.

The reduced stigma growth in flowers with down-regulation of *PhTPS1* by RNA interference, *PhTPS1*-RNAi (*tps1*), could be a result of a direct effect of VOCs on reproductive organ development or indirect consequence of either increased growth of colonizing bacteria or their products on transgenic pistils (*3*). Therefore, *tps1* pistils were treated with bleach for a short time—which, although leaving pistils alive, effectively reduced bacterial levels (fig. S1A)—and were grown within wild-type (WT) or *tps1* tubes. Independent of treatment, *tps1* pistils grown within *tps1* tubes exhibited a reduced stigma size phenotype relative to those grown within WT tubes (fig. S1B), which suggests that the terpenoid signal released from tubes is required for normal pistil development independent of the stigma microbial community.

VOC affects stigma size through a karrikin-like signaling pathway

To determine the molecular mechanisms that underlie interorgan VOC perception and signaling, we generated RNA sequencing (RNA-seq) datasets from WT and *tps1* stigmas on day −1 and day +1 postanthesis. Only minor differences were observed on day −1 postanthesis in transgenics versus WT, whereas comparative analysis of transcript abundances on day +1 showed ~4-fold increase in the number of differentially expressed genes (fig. S2A). Gene Ontology (GO) enrichment analysis revealed that eight out of 23 GO terms (~35%) that were enriched among down-regulated genes were associated with multiple stress responses, including those to ethylene and its upstream regulator karrikin (*18*) (fig. S2B). Therefore, we hypothesized that a karrikin-like signaling pathway is involved in VOC-mediated communication.

Karrikins are not endogenously produced by plants but are bioactive compounds of smoke, which stimulate the gemination of seeds across more than 1200 plant species from more than 80 genera (*15*, *16*). They also regulate numerous plant developmental processes unrelated to fires, including ethylene-dependent root growth (*18*), in addition to their important roles in biotic and abiotic responses (*19*). Karrikins are perceived by the karrikin insensitive2 (KAI2) receptor (*14*, *20*), for which most angiosperms have one or more copies of the encoding gene (s). The widespread occurrence of genes for karrikin responses in plant species from non–fire-prone environments, their evolutionary conservation among the angiosperms, and the origin of KAI2-like proteins before land plant evolution (because they already exist in charophytes) (*21*–*23*) imply that the core function of the karrikin signaling pathways is to sense endogenous KAI2 ligand(s), the nature of which is still unknown (*14*, *15*, *20*).

GO term analysis identified eight genes belonging to "response to karrikin" (GO:0080167) that were down-regulated in the *tps1* mutant relative to WT in our RNA-seq datasets (fig. S3A). By contrast, the expression of petunia

[1]Department of Horticulture and Landscape Architecture, Purdue University, West Lafayette, IN 47907, USA. [2]Department of Plant Biology, College of Biological Sciences, University of California–Davis, Davis, CA 95616, USA. [3]Purdue Center for Plant Biology, Purdue University, West Lafayette, IN 47907, USA. [4]Department of Biochemistry, Purdue University, West Lafayette, IN 47907, USA. [5]Department of Chemistry, Purdue University, West Lafayette, IN 47907, USA. [6]Department of Medicinal Chemistry and Molecular Pharmacology, Purdue University, West Lafayette, IN 47907, USA. [7]Purdue Institute for Cancer Research, Purdue University, West Lafayette, IN 47907, USA. [8]Université Jean Monnet Saint-Etienne, CNRS, LBVpam UMR 5079, F-42023 Saint-Etienne, France.
***Corresponding author. Email: dudareva@purdue.edu**
†Present address: Division of Biochemistry, Interdisciplinary Plant Group, University of Missouri, Columbia, MO 65211, USA.

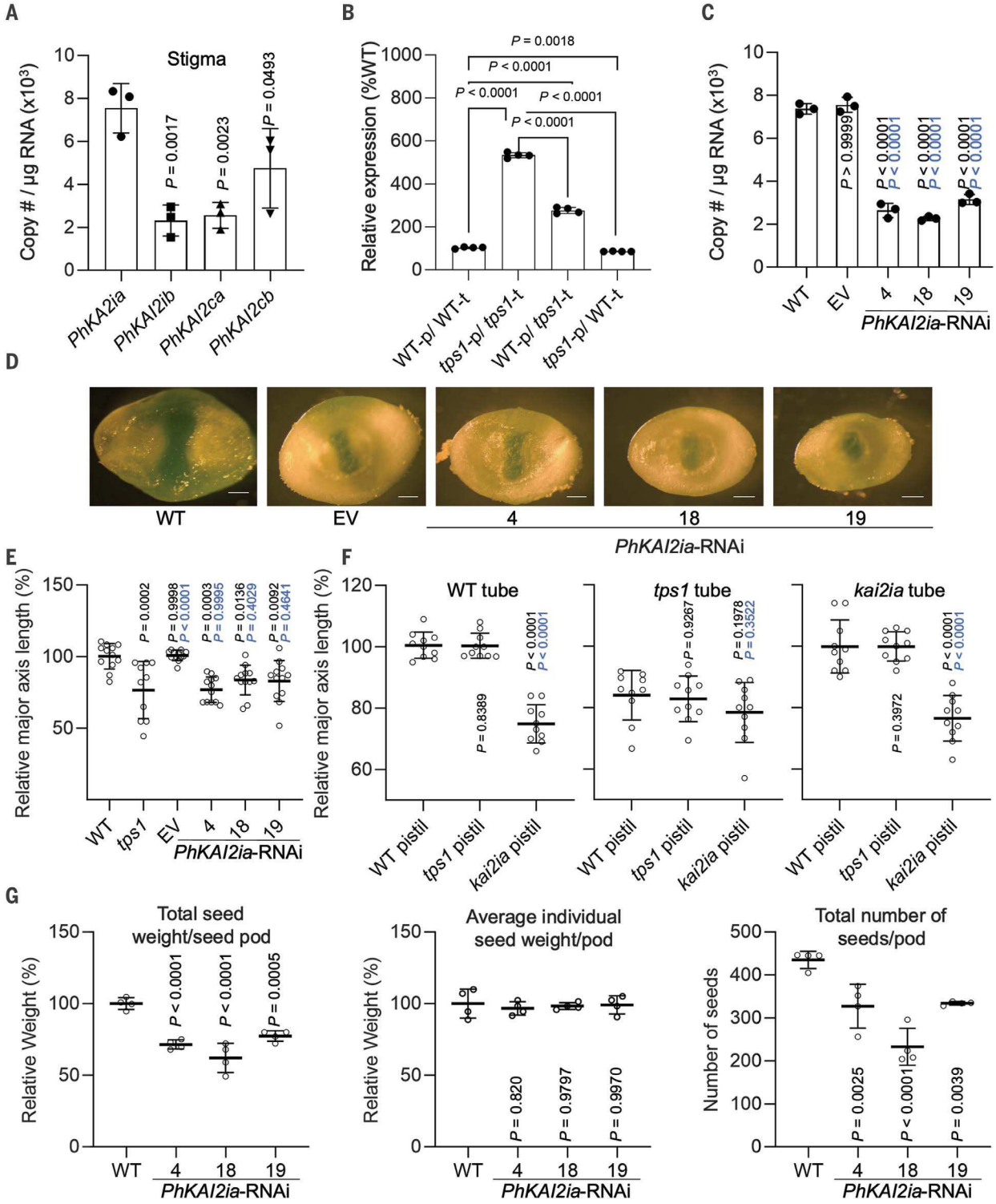

Fig. 1. *PhKAI2ia* is required for sesquiterpene perception and response in petunia stigmas. (**A** to **C**) Expression in stigmas of *PhKAI2s* (A), *PhKAI2ia* within reconstituted flowers of pistil and tube (p/t) genotype combinations (B), and *PhKAI2ia* in WT, empty vector control (EV), and *PhKAI2ia*-RNAi lines (C). In (A) to (C), *P* values were determined by two-way analysis of variance (ANOVA) and Dunnett's multiple comparisons test. In (C), *P* values are relative to WT (black) and EV (blue). *tps1*, *PhTPS1*-RNAi. (**D**) Cross sections of representative stigmas on day 1 postanthesis. Scale bars are 300 µm. (**E**) Stigma major axis length in WT, *tps1*, EV, and *PhKAI2ia*-RNAi lines on day 1 postanthesis normalized to WT. (**F**) Stigma major axis length of WT, *tps1*, and *PhKAI2ia*-RNAi line 18 (*kai2ia*) pistils grown in tubes of WT (left), *tps1* (middle), and *kai2ia* (right) normalized to WT pistils in WT tubes. In (E) and (F), *P* values were determined by two-way ANOVA with Dunnett's multiple comparisons test relative to WT (black) and *tps1* (blue) stigmas within each panel. (**G**) Seed production in *PhKAI2ia-RNAi* lines. *P* values were determined by one-way ANOVA with Tukey's multiple comparison test relative to WT. Data are means ±SD [n = 3 biological replicates in (A) to (C), n = 10 to 12 in (E), n = 10 in (F), and n = 4 in (G)].

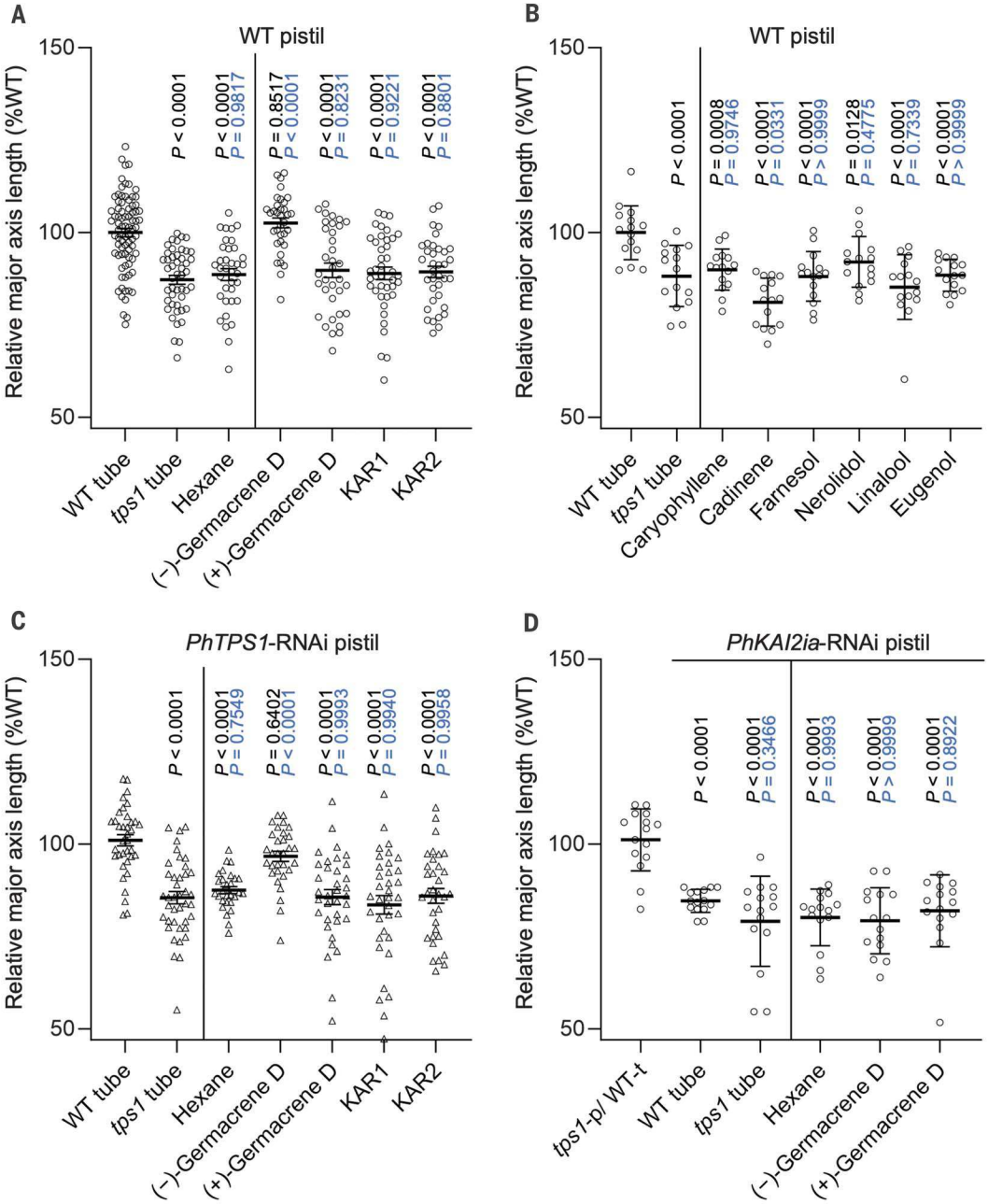

Fig. 2. Pistil growth phenotype response is specific to (−)-germacrene D. (**A** to **D**) Stigma major axis length of WT [(A) and (B)], *PhTPS1*-RNAi (*tps1*) (C), and *PhKAI2ia*-RNAi (line 18) (D) pistils grown in WT and *tps1* tubes as well as in the presence of the volatiles shown on the *x* axis. Results are presented relative to WT pistil growth within WT tubes [(A) and (B)] and *tps1* pistil growth in WT tubes [(C) and (D)] set as 100%. Data are means ±SE in (A) and (C) and ±SD in (B) and (D) [n = 35 to 47 biological replicates in (A), n = 15 in (B), n = 29 to 41 in (C), and n = 15 in (D)]. P values were determined by two-way ANOVA with Dunnett's multiple comparisons test relative to the WT (black) and *tps1* (blue) tubes in (A) to (C) and relative to the *tps1* (black) and *PhKAI2ia*-RNAi (line 18) (blue) pistils grown in the WT tubes in (D). KAR1 and KAR2 indicate karrikins 1 and 2, respectively. Hexane was used as a solvent control.

homologs of known karrikin signaling pathway genes remained largely unchanged, with the exception of *KAI2ia* (fig. S3B). Using identified differentially expressed genes as markers of volatile signal response, we analyzed their transcript levels by quantitative real-time polymerase chain reaction (qRT-PCR) in WT and *tps1* stigmas grown within different volatile conditions. All eight genes were strongly down-regulated upon VOC depletion in *tps1* and WT pistils grown within *tps1* tubes relative to WT pistils grown within WT tube controls (fig. S4A). Moreover, complementation of *tps1* stigmas by fumigation with volatiles emitted by WT tubes (*3*) restored, to a different extent, expression of karrikin-responsive genes, which implies that VOC and karrikin signaling may share similar molecular mechanisms.

PhKAI2ia is required for VOC perception and response

Unlike most angiosperms, the *KAI2* genes in the Lamiids, which make up ~15% of all flowering plants, including Solanales (*24*), form three subclades: conserved (*KAI2c*), intermediate (*KAI2i*), and divergent (*KAI2d*) (*25*–*27*). Like other members of the Solanaceae family, the petunia genome contains four *KAI2* genes, two of which belong to the conserved (*PhKAI2c*) clade and two to the intermediate (*PhKAI2i*) (fig. S5). Out of the four *KAI2* genes, *PhKAI2ia* expression was highest in the stigma based on qRT-PCR analysis (Fig. 1A) and was dependent on VOC levels. It was up-regulated in the reduced VOC environment within *tps1* tubes (Fig. 1B and fig. S4B), which highlights its likely role in sensing volatiles. Therefore, to investigate whether the VOC signaling pathway relies on the KAI2ia receptor, we generated "deaf" receivers by RNAi down-regulation of *PhKAI2ia* under the control of cauliflower mosaic virus 35S promoter. Three independent homozygous lines with 57 to 70% reduced *PhKAI2ia* transcript levels (Fig. 1C) displayed a smaller stigma size phenotype (Fig. 1, D and E) similar to that in

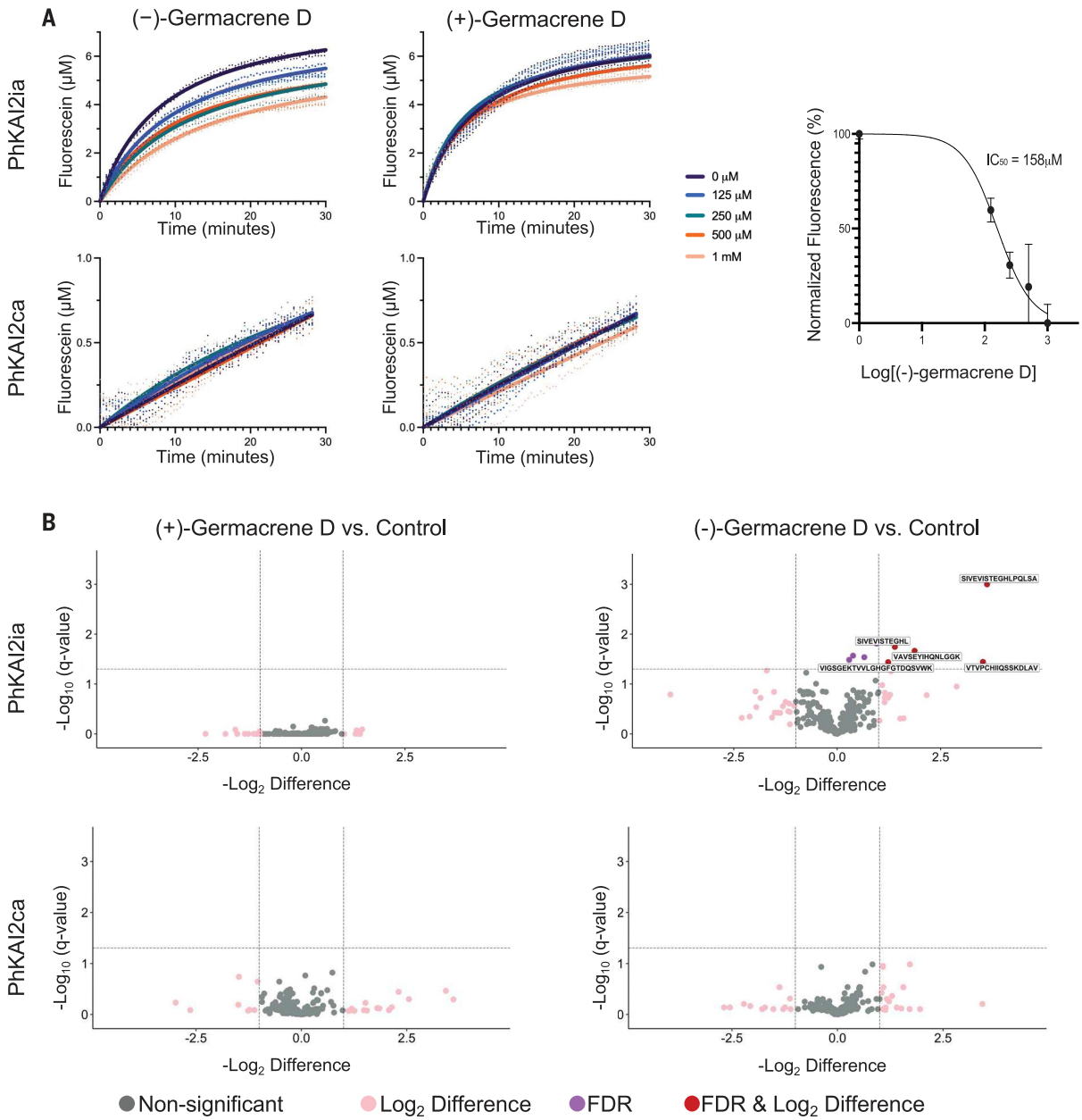

Fig. 3. PhKAI2ia binds specifically to (−)-germacrene D. (**A**) Kinetics of YLG hydrolysis by PhKAI2ia and PhKAI2ca in the presence of (+)- and (−)-germacrene D. Colored lines represent the nonlinear regression curve fit, with data points for triplicates shown in dots (data S2). The inhibitory dose-response curve for (−)-germacrene D is shown on the right. One-way ANOVA and Tukey's test were used to determine significant differences between runs with different germacrene D concentrations. Only PhKAI2ia samples with (−)-germacrene D showed significant differences relative to 0 μM control, with the following *P* values at the indicated (−)-germacrene D concentration: 125 μM, $P \leq 0.05$; 250 μM, $P \leq 0.0001$; 500 μM, $P \leq 0.0001$; and 1 mM, $P \leq 0.0001$. All other comparisons showed no significant differences except when 1 mM (+)-germacrene D was added to PhKAI2ia ($P \leq 0.05$). (**B**) Conformational changes in PhKAI2ia and PhKAI2ca upon incubation with (+)- and (−)-germacrene D as determined by LiP-MS and visualized by volcano plots. Each point represents a peptide. For each protein and condition, a total of 303 peptides were identified, which provided 100% protein coverage. Peptides passing the significance cutoff [$|\log_2(\text{difference})| > 1$ and *q* value < 0.05, as determined by Student's *t* test and a permutation test] are colored in red. FDR, false discovery rate. Single-letter abbreviations for the amino acid residues are as follows: A, Ala; C, Cys; D, Asp; E, Glu; F, Phe; G, Gly; H, His; I, Ile; K, Lys; L, Leu; N, Asn; P, Pro; Q, Gln; S, Ser; T, Thr; V, Val; W, Trp; and Y, Tyr.

tps1 transgenic plants (Fig. 1E). However, unlike *tps1* flowers (*3*), the terpenoid emission from tubes of *PhKAI2ia*-RNAi flowers were not statistically different from that of WT and empty-vector control (fig. S6). In addition, *PhKAI2ia* tubes were able to sustain normal growth of WT stigmas and recover the reduced size of *tps1*, but not *kai2ia*, stigmas (Fig. 1F, right). Moreover, the small *PhKAI2ia* pistil phenotype was independent of tube VOC production (Fig. 1F), and *PhKAI2ia*-RNAi down-regulation did not affect expression of other *PhKAI2* genes—*PhKAI2ca*, *PhKAI2cb*, and *PhKAI2ib*—in transgenic *PhKAI2ia* pistils (fig. S7). Taken together, these results provide genetic evidence for the involvement of PhKAI2ia in the perception of volatile signal(s). They also show that other *PhKAI2* genes, which exhibit varying tissue-

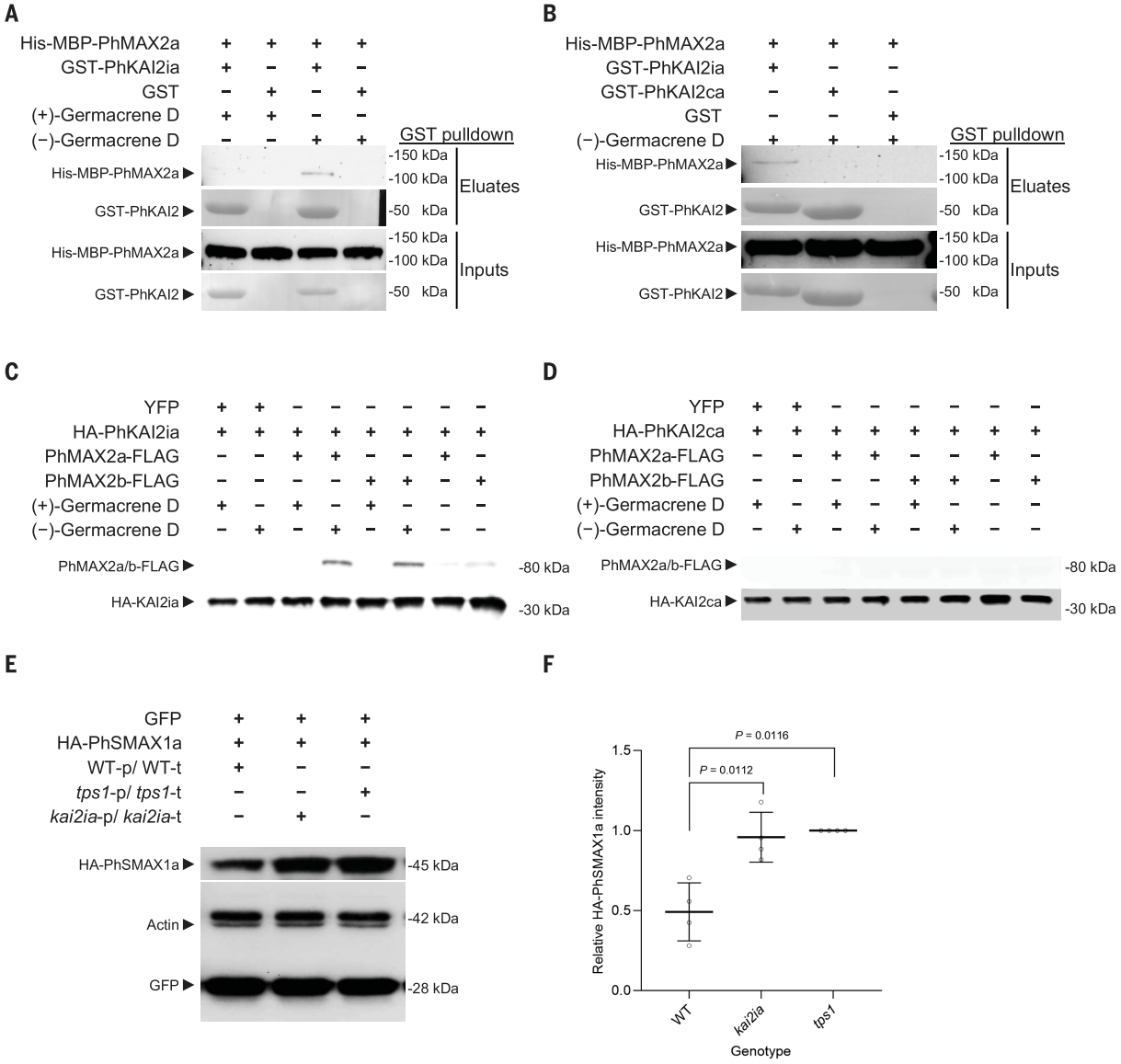

Fig. 4. (−)-Germacrene D is required for PhKAI2ia-PhMAX2 complex formation and PhSMAX1 degradation. (**A** and **B**) In vitro glutathione *S*-transferase (GST) pull down of GST-PhKAI2ia and His-MBP-PhMAX2a (A) and GST-PhKAI2ia, GST-PhKAI2ca, and His-MBP-PhMAX2a (B) in the presence or absence of (+)- or (−)-germacrene D. (**C** and **D**) In vivo complex formation shown by hemagglutinin (HA) pull down of HA-PhKAI2ia (C) and HA-PhKAI2ca (D) with PhMAX2a-FLAG, PhMAX2b-FLAG, or yellow fluorescent protein (YFP) from WT petunia stigmas transiently expressing respective proteins and grown in the presence of (+)- or (−)-germacrene D. YFP was used as a negative control for the specificity of PhKAI2 interactions. (**E**) HA pull down of HA-PhSMAX1a from WT, *tps1*, and *kai2ia* (line 18) petunia stigmas transiently expressing HA-PhSMAX1a and GFP as expression control and grown in tubes of the same genetic background. Actin is shown as a loading control. Proteins were visualized by Western blots with anti-His and anti-GST [(A) and (B)], anti-HA and anti-FLAG [(C) and (D)], and anti-HA antibodies and anti-GFP (E) antibodies as indicated. (**F**) Quantification of PhSMAX1a degradation in different genetic backgrounds. The level of HA-PhSMAX1a was normalized to coexpressed green fluorescent protein (GFP) and presented as means ±SD [n = 4 biological replicates, including one in (E)]. P values were determined by a two-tailed paired Student's t test relative to WT.

specific expression profiles (fig. S8) and encode proteins with 74 to 84% amino acid identity to PhKAI2ia (fig. S5), are unable to compensate for the reduced PhKAI2ia activity, likely because of different ligand binding specificity. Similar to *tps1* flowers, which lack terpene fumigation (*3*), the inability of transgenic *PhKAI2ia*-RNAi plants to perceive the volatile signal affected seed production by reducing the number of seeds by 23 to 47% per flower without affecting the individual seed weight (Fig. 1G), which indicates the decreased fitness in the absence of normal volatile perception.

PhKAI2ia stereospecifically perceives (−)-germacrene D

To determine whether the reproductive organ growth-promoting effect is a distinctive property of (i) (−)-germacrene D, the major product of PhTPS1 (fig. S9), (ii) volatile sesquiterpenes or volatile monoterpenes as classes of compounds, or (iii) volatiles in general, we performed gas phase complementation assays. WT stigmas were grown in the presence of (−)- and (+)-germacrene D because these two enantiomers are known to possess different bioactivities (*28*, *29*); sesquiterpenes cadinene, the most abundant VOC detected in petunia pistils (*3*), caryophyllene, farnesol, and nerolidol; monoterpene linalool; and phenylpropene eugenol. Karrikins (KAR_1 and KAR_2) were also included in these fumigation experiments to determine whether, after being taken in by

pistils (fig. S10), these compounds influence petunia stigma growth. Out of the tested compounds, only (−)-germacrene D was able to promote normal growth of WT pistils (Fig. 2, A and B) and restore the normal stigma size phenotype in *tps1* (Fig. 2C), but not in "deaf" *kai2ia* (Fig. 2D), pistils. Moreover, expression analysis of petunia karrikin-responsive genes in reconstructed flowers with WT pistils fumigated with (−)- and (+)-germacrene D revealed that only the (−)-enantiomer was able to sustain mRNA at levels similar to those in pistils grown within WT tubes (fig. S11A). Exceptions included the *PhSTS* gene, which was up-regulated in response to (−)-germacrene D, and the *PhCRR55* and *PhO04544* genes, the mRNA levels of which were only partially restored. Similar to treatment with tubes from different genotypes (Fig. 1B), *PhKAI2ia* gene expression in pistils was sensitive to the presence of airborne (−)-germacrene D around the pistil, with expression being the highest in the absence of this sesquiterpene (fig. S11B). In contrast to *PhKAI2ia*, expression of *PhKAI2ib*, *PhKAI2ca*, and *PhKAI2cb* remained unaffected by fumigation treatments, which suggests that other petunia KAI2 receptors are insensitive to (−)-germacrene D (fig. S11B).

To biochemically analyze and directly test for ligand affinity, displacement hydrolysis assays with Yoshimulactone Green (YLG), differential scanning fluorimetry (DSF), and limited proteolysis–mass spectrometry (LiP-MS) (fig. S12) (*30*) were performed with purified recombinant PhKAI2ia and PhKAI2ca (fig. S13) in the presence of (−)- and (+)-germacrene D. PhKAI2ca was chosen for these experiments as a representative of the conserved clade (fig. S5), and its encoding gene exhibits the second highest expression in the stigma out of four petunia *PhKAI2*s (Fig. 1A). Notably, PhKAI2ia hydrolysis activity was affected by a wide range of concentrations of (−)-germacrene D and only by high nonphysiological concentrations of the (+)-enantiomer (Fig. 3A). PhKAI2ca hydrolysis activity was comparatively low and not affected by either (−)- or (+)-germacrene D. The calculated median inhibitory concentration (IC_{50}) of 158 μM (measured as normalized percentages of fluorescein product release) shows a (−)-germacrene D dose-dependent inhibition response of PhKAI2ia and is in the range of the (−)-germacrene D concentration (>60 μM) estimated on the basis of its pool size in petunia stigmas (*3*). Interestingly, GR24, a synthetic strigolactone analog, also inhibited YLG hydrolysis by both PhKAI2 receptors (fig. S14).

DSF showed no thermal shift of either PhKAI2ia or PhKAI2ca in the presence of (−)- and (+)-germacrene D, possibly because of known limitations of this technique with volatile ligands (*27*, *31*, *32*) (fig. S15). Thus, we used LiP-MS, another widely used method to identify protein–small molecule interactions and validated it by using AtKAI2 with one of its known ligands, (−)-GR24 (fig. S16). LiP-MS identified 300 peptides for both PhKAI2s, covering the entirety of each protein. Only PhKAI2ia exhibited conformational changes when treated with (−)-germacrene D, which resulted in significant increases in the intensities of five peptides as compared to either PhKAI2ia treated with (+)-germacrene D or PhKAI2ca samples treated with (−)- or (+)-germacrene D (Fig. 3B). Modeling of the PhKAI2ia structure by AlphaFold2 (*33*) (fig. S17A) followed by docking with (−)-germacrene D and molecular dynamics simulations (fig. S17B) revealed a conserved ligand-binding pocket that coordinates the docked (−)-germacrene D within the active site (fig. S17, C to E). About 17 amino acids within the pocket, including Gly^{25}, Phe^{26}, catalytic Ser^{95}, Leu^{96}, Phe^{124}, Phe^{134}, Leu^{142}, Phe^{157}, Val^{161}, Phe^{174}, Ile^{193}, Phe^{194}, Leu^{218}, Ala^{219}, Val^{220}, catalytic His^{246}, and Leu^{247} coordinate the interaction with (−)-germacrene D (fig. S17, C to F). Several of these residues were previously found to not only coordinate other synthetic ligands like GR24 but also help differentiate ligand sensitivity (*34*–*37*). These structurally altered sequences (shown in boxes) were located near the N- and C-terminal regions of PhKAI2ia and

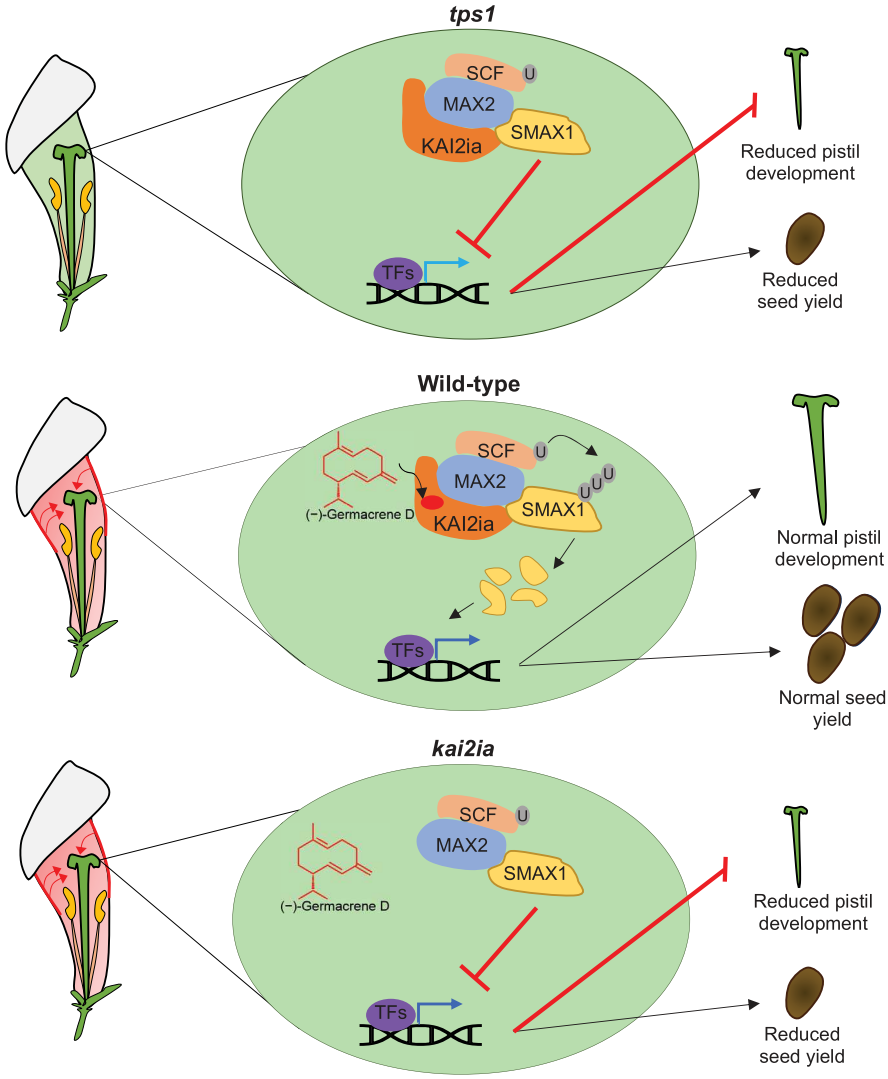

Fig. 5. Proposed model for (−)-germacrene D KAI2ia-dependent signaling in petunia pistils. Under normal WT growth conditions (middle), KAI2ia perceives (−)-germacrene D, which leads to the recruitment of MAX2a and/or MAX2b and the subsequent targeting of SMAX1a for degradation, resulting in normal pistil development and seed yield. Under *tps1* RNAi knockdown conditions (top), the decreased (−)-germacrene D signal ("mute emitters") reduces KAI2ia-MAX2 complex formation and SMAX1a degradation, resulting in smaller pistils and lower seed yield relative to WT plants. Under *kai2ia* RNAi knockdown conditions (bottom), less complex formation occurs because of a diminished ability to perceive (−)-germacrene D signal ("deaf receivers"), which results in similar pistil and seed phenotypes, as in "mute emitters." TFs, transcription factors; U, ubiquitin.

found to coincide with the potential binding sites of (−)-germacrene D that were determined by the simulation results (fig. S17F).

PhKAI2ia-mediated VOC signaling requires MAX2 proteins

Sensing a signal is a crucial first step in communication, yet the subsequent downstream transduction events that occur upon perception are equally critical to propagating cellular changes. Studies have shown that MAX2, an F-box protein of the SKP1-CUL1-F-box (SCF) E3 ubiquitin ligase complex, is an essential part of both strigolactone and karrikin signaling (*38–40*), which mediates the ubiquitination and proteasomal degradation of transcriptional repressors (*39*, *41–44*). Like other members of the Lamiids, which contain the distinctive KAI2i clade, petunia has two copies of *MAX2* genes that are ubiquitously expressed across aerial plant tissues and encode proteins PhMAX2a and PhMAX2b with 81% amino acid identity (fig. S18). To investigate whether PhKAI2ia-mediated VOC signaling shares common molecular mechanisms with the strigolactone and karrikin pathways and acts through MAX2 protein(s), we analyzed the subcellular localization of potential interactors. Fluorescently tagged fusion proteins PhKAI2ia and PhKAI2ca, when transiently expressed in *Arabidopsis* protoplasts (fig. S19) and *Nicotiana benthamiana* leaves (fig. S20), showed dual localization in the nucleus and cytoplasm similar to their *Arabidopsis* homologs (*45*). As predicted (*39*), PhMAX2a showed localization primarily to the nucleus, whereas PhMAX2b demonstrated dual localization in the nucleus and cytoplasm when expressed in protoplasts (fig. S19). Taken together, these results suggest that PhKAI2ia and PhKAI2ca co-occur with PhMAX2a and PhMAX2b in the nucleus, allowing potential interactions. In addition, the co-occurrence of PhMAX2b with PhKAI2ia and PhKAI2ca in the cytoplasm suggests a previously unexplored role of a MAX2 in this compartment.

To determine whether PhKAI2ia forms a complex with PhMAX2a and/or PhMAX2b and the role of (−)- germacrene D in these interactions, pull-down experiments in vitro and in vivo were performed using tagged PhKAI2ia and PhKAI2ca with PhMAX2a and PhMAX2b in the presence of (−)- and (+)-germacrene D. Our in vitro results with recombinant PhMAX2a produced in baculovirus-insect cells (fig. S21) show that (i) PhKAI2ia interacts with PhMAX2a in the presence of (−)-germacrene D but not (+)-germacrene D (Fig. 4A) and that (ii) this interaction is specific for PhKAI2ia and does not occur with PhKAI2ca (Fig. 4B). Additionally, (−)-germacrene D facilitates in vivo complex formation between PhKAI2ia and PhMAX2a as well as PhMAX2b (Fig. 4C), whereas no interactions were detected when *PhKAI2ca* was transiently overexpressed in petunia stigmas instead of *PhKAI2ia* (Fig. 4D).

(−)-Germacrene D promotes degradation of transcriptional co-repressor SMAX1

It is well established that karrikins induce the degradation of known signaling repressor SUPPRESSOR OF MAX2 1 (SMAX1) upon interaction with the KAI2 receptor, which leads to the activation of a downstream signaling cascade (*46–48*). To test whether SMAX1 degradation is involved in (−)-germacrene D–mediated PhKAI2ia signaling, we analyzed the degradation of both PhSMAX1a and PhSMAX1b upon transient expression in stigmas of different petunia backgrounds: WT, *tps1* mutants ("mute emitters"), and *kai2ia* transgenics ("deaf receivers") of their D2 domains that were previously shown to be sufficient in strigolactone and karrikin signaling (fig. S22) (*44*, *46*, *49*). The deficiency in (−)-germacrene D signal, either because of a compromised perception in *kai2ia* stigmas or an inability to produce signal in *tps1* tubes, resulted in no PhSMAX1a degradation, in contrast to a 51% decrease in PhSMAX1a levels in WT stigmas, which were naturally fumigated by volatiles produced in flower tubes (Fig. 4, E and F). No volatile-dependent degradation of PhSMAX1b was found in the analyzed petunia backgrounds (fig. S23), which suggests that unlike PhSMAX1a, PhSMAX1b is not involved in (−)-germacrene D signaling.

Conclusions

Using the hormone-like function of volatile terpenoids in petunia reproductive organ development as a system with a visual marker for communication, we provide strong evidence that (i) perception of volatiles is compound specific and affects plant fitness; (ii) out of four *PhKAI2* genes, only expression of *PhKAI2ia* negatively correlates with the levels of emitted terpenoids; (iii) PhKAI2ia, a karrikin-insensitive receptor of a distinctive intermediate clade stereospecifically recognizes (−)-germacrene D; (iv) (−)-germacrene D–mediated communication relies on the KAI2ia-dependent signaling pathway and shares some transcriptional gene targets with the karrikin responses; and (v) the KAI2ia-dependent (−)-germacrene signal transduction operates through PhMAX2 ubiquitin ligase degradation of PhSMAX1a, and other PhKAI2 receptors are unable to compensate for reduced PhKAI2ia activity (Fig. 5). Although (−)-germacrene D represents a potential karrikin-like ligand and can bind the PhKAI2ia receptor, mediates formation of the PhKAI2ia-PhMax2 complex, and facilitates signal transduction through PhSMAX1a degradation, it does not contain a butenolide moiety shared by karrikins and strigolactones (*15*, *16*, *50*). Because gas complementation and pull-down assays were performed in vivo, it is possible that (−)-germacrene D is metabolized by endogenous enzymes in planta to a more potent ligand for the PhKAI2ia receptor, which requires further investigation. Many plants produce germacrene; however, its production in most species is dominated by (−)-germacrene D (*51*). Interestingly, in addition to the existence of a specific plant receptor for (−)-germacrene D described here, heliothine moths possess neurones with high sensitivity and selectivity to (−)-germacrene D (*28*, *52*). This highlights the importance of this compound not only for within-plant communication but also in a broader ecological context for plant-insect interactions.

REFERENCES AND NOTES

1. A. C. Vlot, M. Rosenkranz, *J. Exp. Bot.* **73**, 445–448 (2022).
2. H. Bouwmeester, R. C. Schuurink, P. M. Bleeker, F. Schiestl, *Plant J.* **100**, 892–907 (2019).
3. B. Boachon *et al.*, *Nat. Chem. Biol.* **15**, 583–588 (2019).
4. J. Midzi *et al.*, *Plants* **11**, 2566 (2022).
5. A. Russo, S. Pollastri, M. Ruocco, M. M. Monti, F. Loreto, *J. Plant Interact.* **17**, 840–852 (2022).
6. F. Adebesin *et al.*, *Science* **356**, 1386–1388 (2017).
7. P. Liao *et al.*, *Nat. Chem. Biol.* **17**, 138–145 (2021).
8. P. Liao *et al.*, *Nat. Commun.* **14**, 330 (2023).
9. Y. Jiang, H. Matsunami, *Curr. Opin. Neurobiol.* **34**, 54–60 (2015).
10. D. Urano, A. M. Jones, *Annu. Rev. Plant Biol.* **65**, 365–384 (2014).
11. C. Xie *et al.*, *Plant J.* **33**, 385–393 (2003).
12. R. F. Lacey, B. M. Binder, *J. Inorg. Biochem.* **133**, 58–62 (2014).
13. Q. Gong *et al.*, *Nature* **622**, 139–148 (2023).
14. M. T. Waters *et al.*, *Development* **139**, 1285–1295 (2012).
15. D. C. Nelson, G. R. Flematti, E. L. Ghisalberti, K. W. Dixon, S. M. Smith, *Annu. Rev. Plant Biol.* **63**, 107–130 (2012).
16. G. R. Flematti, E. L. Ghisalberti, K. W. Dixon, R. D. Trengove, *Science* **305**, 977–977 (2004).
17. A. Nagashima *et al.*, *J. Biol. Chem.* **294**, 2256–2266 (2019).
18. S. M. Swarbreck, *Trends Plant Sci.* **26**, 308–311 (2021).
19. M. T. Waters, D. C. Nelson, *New Phytol.* **237**, 1525–1541 (2023).
20. G. R. Flematti, K. W. Dixon, S. M. Smith, *BMC Biol.* **13**, 108 (2015).
21. R. Bythell-Douglas *et al.*, *BMC Biol.* **15**, 52 (2017).
22. C. H. Walker, K. Siu-Ting, A. Taylor, M. J. O'Connell, T. Bennett, *BMC Biol.* **17**, 70 (2019).
23. P.-M. Delaux *et al.*, *New Phytol.* **195**, 857–871 (2012).
24. N. F. Refulio-Rodriguez, R. G. Olmstead, *Am. J. Bot.* **101**, 287–299 (2014).
25. C. E. Conn *et al.*, *Science* **349**, 540–543 (2015).
26. G. Xiong, J. Li, S. M. Smith, *Mol. Plant* **9**, 493–495 (2016).
27. Y. K. Sun *et al.*, *Nat. Commun.* **11**, 1264 (2020).
28. M. Stranden, A. K. Borg-Karlson, H. Mustaparta, *Chem. Senses* **27**, 143–152 (2002).
29. I. Prosser *et al.*, *Arch. Biochem. Biophys.* **432**, 136–144 (2004).
30. S. Schopper *et al.*, *Nat. Protoc.* **12**, 2391–2410 (2017).
31. M. T. Waters *et al.*, *Plant Cell* **27**, 1925–1944 (2015).
32. J. Yao *et al.*, *Plant J.* **96**, 75–89 (2018).
33. M. Mirdita *et al.*, *Nat. Methods* **19**, 679–682 (2022).
34. S. Carbonnel *et al.*, *PLOS Genet.* **16**, e1009249 (2020).
35. A. M. Guercio *et al.*, *Commun. Biol.* **5**, 126 (2022).
36. A. M. Guercio, M. Palayam, N. Shabek, *Phytochem. Rev.* **22**, 339–360 (2023).
37. S. E. Martinez *et al.*, *Plant Physiol.* **190**, 1440–1456 (2022).
38. D. C. Nelson *et al.*, *Proc. Natl. Acad. Sci. U.S.A.* **108**, 8897–8902 (2011).
39. P. Stirnberg, I. J. Furner, H. M. Ottoline Leyser, *Plant J.* **50**, 80–94 (2007).
40. M. T. Waters, C. Gutjahr, T. Bennett, D. C. Nelson, *Annu. Rev. Plant Biol.* **68**, 291–322 (2017).
41. L. Jiang *et al.*, *Nature* **504**, 401–405 (2013).
42. J. P. Stanga, S. M. Smith, W. R. Briggs, D. C. Nelson, *Plant Physiol.* **163**, 318–330 (2013).
43. I. Soundappan *et al.*, *Plant Cell* **27**, 3143–3159 (2015).
44. N. Shabek *et al.*, *Nature* **563**, 652–656 (2018).
45. X.-D. Sun, M. Ni, *Mol. Plant* **4**, 116–126 (2011).
46. A. Khosla *et al.*, *Plant Cell* **32**, 2639–2659 (2020).
47. J. Zheng *et al.*, *Plant Cell* **32**, 2780–2805 (2020).
48. Y.-J. Park, J. Y. Kim, C.-M. Park, *Plant Cell* **34**, 2671–2687 (2022).
49. L. Tal *et al.*, *New Phytol.* **239**, 2067–2075 (2023).
50. A. de Saint Germain *et al.*, *Nat. Chem. Biol.* **12**, 787–794 (2016).
51. N. Bülow, W. A. König, *Phytochemistry* **55**, 141–168 (2000).

52. M. Stranden *et al*., *J. Comp. Physiol. A Neuroethol. Sens. Neural Behav. Physiol.* **189**, 563–577 (2003).
53. A. Bombarely *et al*., *Nat. Plants* **2**, 16074 (2016).

ACKNOWLEDGMENTS

Funding: This work was supported by National Science Foundation IOS grant 2139804 to N.D. and N.S.; US Department of Agriculture (USDA) National Institute of Food and Agriculture Hatch Project numbers 177845 and 1013620 to N.D. and Y.L., respectively; USDA National Institute of Food and Agriculture Postdoctoral grant 2019-67012-29660 to R.M.P.; CNRS IEA and AAP Université Jean Monnet grants to B.B.; and NIH grant 3RF1AG064250 to W.A.T. We thank J. H. Lynch for isolation of two RNA samples for RNA-seq. **Author contributions:** N.D. and N.S. conceived the project. S.A.S. generated transgenic plants and performed RNA analysis and complementation assays. A.M.G. performed displacement assays and analyzed protein-protein interactions in vitro. F.S. produced recombinant proteins in insect cells. R.M.P., B.B., M.E.B., and Y.L. generated and analyzed RNA-seq datasets. B.B. analyzed the stereochemistry of germacrene D. X.-Q.H. and V.D. performed subcellular localization. X.-Q.H. and S.A.S. performed phylogenetic analysis. X.-Q.H. and A.M.G. performed modeling. V.D. and R.W.J.K. analyzed protein-protein interactions in planta. Y.-K.L. and W.A.T. performed LiP-MS analysis. N.D. and M.E.B. wrote the manuscript with contributions from all authors. All authors read and edited the manuscript. **Competing interests:** The authors declare no competing interests. **Data and materials availability:** All data are available in the main text or supplementary materials. The generated RNA-seq datasets were deposited in the NCBI Gene Expression Omnibus under GEO accession ID GSE245080, and the sequences reported in this paper have been deposited in the GenBank database as OR700010 to OR700017. *Petunia axillaris* genomic data were obtained from http://solgenomics.net using the *P. axillaris* v1.6.2 genome database (*53*). All peptide MS data have been deposited to the ProteomeXchange Consortium via the jPOST partner repository under reference ID PXD048893.

SUPPLEMENTARY MATERIALS

science.org/doi/10.1126/science.adl4685
Materials and Methods
Figs. S1 to S23
Table S1
References (*54–60*)
MDAR Reproducibility Checklist
Data S1 and S2

Submitted 19 October 2023; accepted 8 February 2024
10.1126/science.adl4685